24th COBEM - 2017

24th ABCM International Congress of Mechanical Engineering
December 3-8, 2017, Curitiba, PR, Brazil

COBEM-2017-0385
NUMERICAL SIMULATION OF TURBULENT FLOW OVER A BACKWARD-FACING STEP

Filipe Alcântara Soares
Priscila Pires Araújo
André Luiz Tenório Rezende
Department of Mechanical and Materials Engineering, IME - Military Engineering Institute, 22290-270, Rio de Janeiro, RJ, Brazil
alcantara_filipe@hotmail.com, priscila.pires.engenergia@gmail.com, arezende@ime.eb.br

Abstract. *The flow over a backward-facing step is a complex case in the scope of computational fluid dynamics, present in several engineering examples. In fact, its complexity is due to adverse pressure gradient which affects a separation of the boundary layer, thus presenting separation, recirculation and reattachment of the flow steps. In the present work all these steps are analyzed numerically in a simplified way through the construction of a case with a simple geometry. To numerically simulate this case, were used Reynolds Average Navier-Stokes equations (RANS) for a two-dimensional steady state flow and the turbulence models used are the k-ω and SST k-ω. The expansion ratio is E_R=2 and the Reynolds number, based on the step height and mean inlet velocity is Re = 9000. Results were compared with data from the literature using direct numerical simulation (DNS). The results for both simulated models were satisfactory and close to those found in direct numerical simulation. The results presented in the SST k-w model are closer to the results expected and found by the use of direct numerical simulation due to their better application in cases involving adverse pressure gradient and boundary layer separation. The main results analyzed in this paper are reattachment length, coefficient of friction, mean velocity and pressure coefficient.*

Keywords: *Backward-Facing Step, Reynolds Averaged Navier-Stokes, k-ω model, Shear-Stress Ttransport k-ω model, reattachment.*

1. INTRODUCTION

The main objective of the present work is the computational analysis of geometry with a backward-facing step. In this situation, the adverse pressure gradient causes the separation of the turbulent boundary layer and this phenomenon has been widely studied in the area of fluid dynamics, since it has a great importance in aerodynamic designs (Lee and Mateescu, 1998). The separation is the result of a slow movement of the fluid adjacent to the wall and the frictional force is of great importance in this process. Therefore, the adverse pressure gradient generates the separation of the flow, in addition to recirculation zones and the subsequent reattachment of the flow, as shown in Fig. 1. These characteristics are found in many engineering cases, such as internal flows in channels and valves, and external flows on airfoils and buildings (Armaly *et al.*, 1983). The present work deals with the construction of a case with a simple geometry that addresses all the above characteristics.

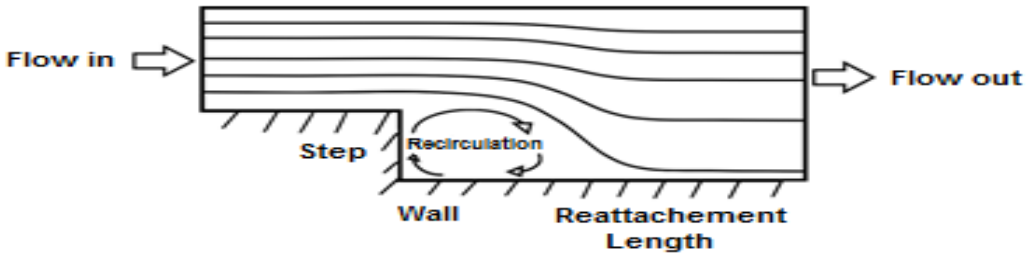

Figure 1. Flow features of backward-facing step flow.

The simulations were accomplished with models based in the Reynolds Average Navier-Stokes equations (*RANS*), with Reynolds number $Re = 9000$. The Reynolds number is defined as a function of the step height, the kinematic viscosity of the fluid and the mean input velocity, given by Eq (1).

$$Re = \frac{U \times h}{\upsilon} \tag{1}$$

The expansion ratio of the simulated cases in the present study is $E_R = 2$. The expansion ratio is a relation between the height of the outlet channel and the height of the step, given by Eq. (2).

$$E_R = \frac{L_y}{L_y - h} \tag{2}$$

The performance of the turbulence models used for the case constructed in the present work is evaluated by comparing the results obtained with the results obtained by Kopera (2011). Kopera (2011) performs a simulation with $Re = UH/\nu = 9000$ and uses a direct numerical simulation (*DNS*) method and an expansion ratio $E_R = 2$.

Based on previous studies, this work presents numerical results of the geometry with a backward-facing step using two different turbulence models of two equations: *k-ω* (Wilcox, 1988) and *SST k-ω* (Menter, 1994). The *SST k-ω* model was used because it presents better results in cases with adverse pressure gradient and flow separation, according to previous work. The *k-ω* model was chosen with the objective of comparing its results with the results of the *SST k-ω* model and both results are compared with the numerical results obtained by Kopera (2011).

2. MATHEMATICAL MODELING

The flow through a channel with a step built in the current work is governed by the application of the Reynolds averages equation method (*RANS*) in the equations that describe the incompressible fluid movement. These equations are momentum equations and continuity, given respectively by

$$\left(\frac{\partial u_i u_j}{\partial x_j}\right) = g_i - \frac{1}{\rho}\frac{\partial p}{\partial x_i} + \frac{\partial}{\partial x_j}\left(\upsilon \frac{\partial u_i}{\partial x_j}\right);\ \frac{\partial u_j}{\partial x_j} = 0 \tag{3}$$

The method of the average Reynolds equations is based on the decomposition of the velocity instantaneous value in $u_i = \overline{u_\iota} + u_i'$, where u_i represents the velocity instantaneous value, $\overline{u_\iota}$ is the mean velocity vector and u_i' represents the velocity fluctuation vector (Rezende, 2009). Thus, the average momentum equation, for steady state and incompressible flow, and the average continuity equation are given by

$$\frac{\partial \overline{u_\iota}\,\overline{u_j}}{\partial x_j} = g_i - \frac{1}{\rho}\frac{\partial \bar{p}}{\partial x_i} + \frac{\partial}{\partial x_j}\left(\nu \frac{\partial \overline{u_\iota}}{\partial x_j} - \overline{u_\iota{}' u_j{}'}\right);\ \frac{\partial \overline{u_j}}{\partial x_j} = 0 \tag{4}$$

The term $\overline{u_\iota{}' u_j{}'}$ is the turbulent Reynolds Stress, which represents the influence of fluctuations in the average flow.

In order to close Eq. (4) it is necessary to determine the values of turbulent Reynolds stresses. These stresses can be found by means of an analogy with Stokes' law, based on the Boussinesq hypothesis, where the turbulent stresses are proportional to the mean flow velocity gradient.

$$-\overline{u_\iota{}' u_j{}'} = \upsilon_t \left(\frac{\partial \overline{u_j}}{\partial x_j} + \frac{\partial \overline{u_j}}{\partial x_i}\right) - \frac{2}{3} k \delta_{ij};\ k = \frac{1}{2}\overline{u_\iota{}' u_\iota{}'} \tag{5}$$

The term υ_t is the turbulent viscosity, defined according to the models. There are several models of turbulence to solve this question and the two models used in this work will be described below.

2.1 *k-ω* Model

In this model, the modeled equation of k is solved together with an equation for the specific rate of turbulent kinetic energy dissipation, resulting in $\omega = \varepsilon/k$. Generally ω is determined to be the characteristic frequency of the turbulence decay process, where its inverse is the time scale at which turbulent energy dissipation occurs. Its rate is determined by the rate of energy transfer over the spectrum of lengths, so ω is defined by the large scales of motion and is closely related to the mean flow properties (Miranda, 2014).

The most commonly used *k-ω* model is Wilcox (1988), which is called the standard *k-ω* model, where the turbulent viscosity is formulated by:

$$v_t = a^* \frac{k}{\omega} \; ; a^* = 1 \tag{6}$$

The Wilcox standard *k-ω* model shows good performance for free shear flows and flow on flat plates with boundary layer, as well as for more complex flows with adverse pressure gradients and separate flows (Wilcox, 1998).

The main negative point of this model is that it presents a strong dependence of the boundary condition on the free current for *ω* (Wilcox, 1991; Menter, 1992). This problem can be avoided by applying boundary conditions for *ω* in the sufficiently large free current, or by applying a minimum value for *ω* across the domain. This method is effective for boundary layer simulations where the *ω* values close to the wall region are close to infinity and, therefore, are not influenced by the *ω* values in the non-turbulent region. However, this solution is not valid for the problem of free shear flows where the values of *ω* within the turbulent region may be of magnitude comparable to the required values of *ω* in the non-turbulent region (Miranda, 2014).

2.2 SST k- ω MODEL

The SST *k-ω* model (Shear-Stress Transport *k-ω*) (Menter, 1994) is widely used in cases with high adverse pressure gradients and boundary layer separation, by means of a combination of *k-ε* and *k-ω* turbulence models (Chitsomboon, 2011). The *k-ω* model presents better results than the *k-ε* model in the solution of the viscous region near the wall, and its results have been satisfactory in cases involving adverse pressure gradients. However, the *k-ω* model requires a non-zero boundary condition for *ω* for non-turbulent free currents, and the calculated flow has a high sensitivity to the specified value (Menter, 1994). It has also been shown (Cazalbou *et al*., 1993) that the *k-ε* model does not exhibit this deficiency. Therefore, the SST *k-ω* model is the robust and precise combination of the *k-ω* model in the region near the walls with the independence of the free current of the *k-ε* model outside the boundary layer. For this, the *k-ε* model is written in terms of the specific dissipation rate, *ω*. Then, the standard *k-ω* model and the modified *k-ε* model are multiplied by a mixing function and summed (Rezende, 2009). The mixing function F_1 is defined as a unite value (considering the standard *k-ω* model) in the inner region of the turbulent boundary layer and is zero (considering the standard *k-ε* model) at the outer edge of the layer.

$$F_1 = tangh(arg_1{}^4) \; ; \; arg_1 = \min\left[max\left(\frac{\sqrt{k}}{\beta^* \omega d}; \frac{500v}{d^2 \omega}\right); \frac{4\sigma_{\omega 2} k}{CD_{k\omega} d^2}\right] \tag{7}$$

$$CD_{k\omega} = \max\left(2\rho\sigma_D \frac{1}{\omega}\frac{\partial k}{\partial x_j}\frac{\partial \omega}{\partial x_j}; 10^{-10}\right) \tag{8}$$

The $CD_{k\omega}$ term is the positive portion of the cross difuse and d is the distance to the nearest surface.

The turbulent viscosity is formulated as follows:

$$v_t = \frac{a_1 \omega}{\max(a_1 \omega; SF_2)} \; ; \; F_2 = tangh(arg_2{}^2) \; ; \; arg_2 = \max\left(\frac{2\sqrt{k}}{\beta^* \omega d}; \frac{500v}{d^2 \omega}\right) \tag{9}$$

The term S refers to the modulus of the tensor average strain rate $\overline{S_{ij}}$, F_2 refers to the mixing function for the turbulent viscosity in the *SST k-ω model* and *d* is the distance to the wall.

The turbulent kinetic energy *k* and the specific dissipation rate *ω* of this model can be obtained by the solution of its conservation equations, where the closing set ϕ for the *SST k-ω* are calculated by the use of a mixing function between the constants ϕ_1 , of the standard k-ω model and ϕ_2 of the model k-ε, making $\phi = F_1\phi_1 + (1 - F_1)\phi_2$. The constants used in the *SST k-ω* model are shown in Tab. 1.

Table 1. SST k-ω model constants.

Constant	ϕ_1	ϕ_2
β	0.0750	0.0828
β^*	0.09	0.09
σ_k	0.5	1.0
σ_ω	0.5	0.856
σ_D	0.856	0.856
α	5/9	0.44

3. METHODOLOGY

The case analyzed in the present work consists of the construction of a 2D geometry simulating the flow inside a channel with a sudden unilateral expansion. The geometry is represented in Fig. 2. The inlet channel has width $L_i = 4h$ and height equal to *h* and the outlet channel has width $L_x = 29h$ and height $L_y = 2h$, where *h* is the height of the step.

The value of *h* used in the simulations performed in the present work is equal to 1 m. Therefore, the expansion ratio is equal 2.

The studies performed by Kopera (2011) indicate that there is a weak dependence of the reattachment length X_R on the Reynolds number in turbulent regime. In this simulation, inlet velocity is 1 m/s, outlet pressure is 0 Pa, kinematic viscosity of the fluid is 0.000111 m^2 s and *h* is equal to 1 m. Therefore, the Reynolds number Re used in this work is the same one used by Kopera (2011) in his simulations, $Re_h = 9000$.

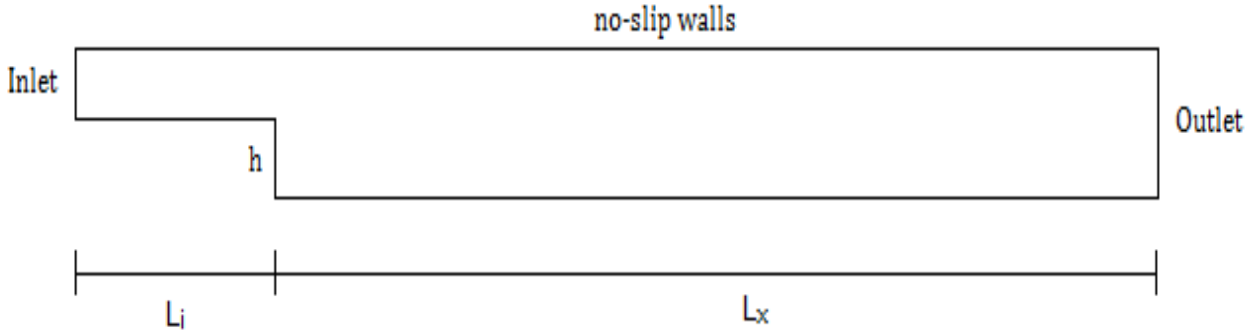

Figure 2. Geometry.

The mesh generated has 155000 elements and 156751 nodes, with a greater refinement in the region near the step.

In all cases simulated in the present work the Finite Volumes Method was used to discretize the government equations. The interpolation scheme used is QUICK (Leonard, 1979) and the SIMPLE scheme was used in the pressure-velocity coupling. For the resolution of the system of linear equations the Multigrid (Hutchinson and Raithby, 1986) technique was used. The problem was considered converged when all residues were lower than 10^{-6}.

The software ANSYS FLUENT® was used to construct the geometry, the meshes and to determine the velocity and pressure coefficient fields.

4. RESULTS

This section presents the results obtained in the simulations of the case treated in this work using *k-ω* and *SST k-ω* turbulence models. The results were compared with the results found by Kopera (2011) in direct numerical simulation. Important parameters for this case are discussed here, such as reattachment length, coefficient of friction, mean velocity and pressure coefficient.

4.1 Reattachment length and coefficient of friction

The reattachment length (X_R) can be determined by the average distance from the step edge to the reattachment position, which can be obtained from the zeros of the coefficient of friction on the bottom wall (Kopera, 2011). Table 2 shows the values of the Reynolds number, expansion ratios and reattachments length of the cases constructed in this work using the two turbulence models, in order to compare the values of X_R with the values of X_R obtained by Kopera (2011).

Table 2. Reattachment length values for the different turbulence models.

Case	Re	E_R	X_R
DNS	9000	2	8.62
k-ω	9000	2	9.83
SST k-ω	9000	2	8.50

Figure 3 shows the comparison between the values of the coefficient of friction found in the simulation with the *k-ω* and *SST k-ω* models and the values of Kopera (2011). These values represent the values of the coefficient of friction in the bottom wall.

Because Kopera (2011) uses the maximum inlet velocity U_0 to scale C_f, was used the mean bulk velocity at the inlet U to set velocity scales, for C_f was used $U_0 = 1.22U$.

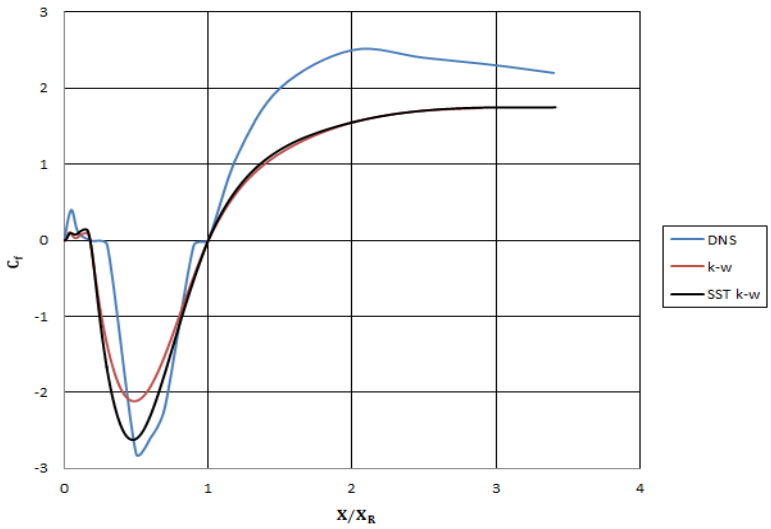

Figure 3. Coefficient of friction at bottom wall.

It can be observed that the results obtained in the cases where the *SST k-ω* model were used presented results closer to the results obtained by Kopera (2011), in relation to the simulated case with the standard *k-ω* model. These results are due to the fact that the *SST k-ω* model is a kind of improvement of the standard *k-ω* model.

4.2 Mean Velocity

Figure 4 shows the velocity contours for both models constructed in this work, where the presence of a primary bubble is observed in the region near the step and then there is the reattachment in the region near *x/h* = 8.60 and regeneration downstream in a fully developed flow in the channel. For the two *RANS* models used, it was possible to observe the presence of a secondary bubble as in the work of Kopera (2011), using the direct numerical simulation model.

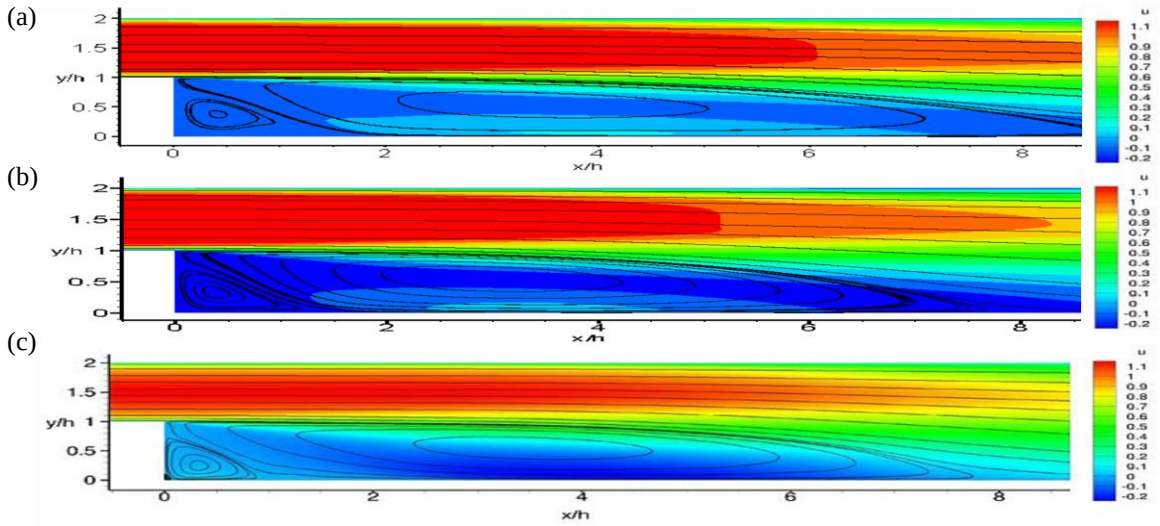

Figure 4. Velocity contours. (a) *k-ω* model. (b) *SST k-ω* model. (c) *DNS*.

The *U* velocity profiles at four different locations are presented in Fig. 5, where it is observed that the results obtained in both *k-ω* and *SST k-ω* models are close to the values obtained by Kopera (2011).

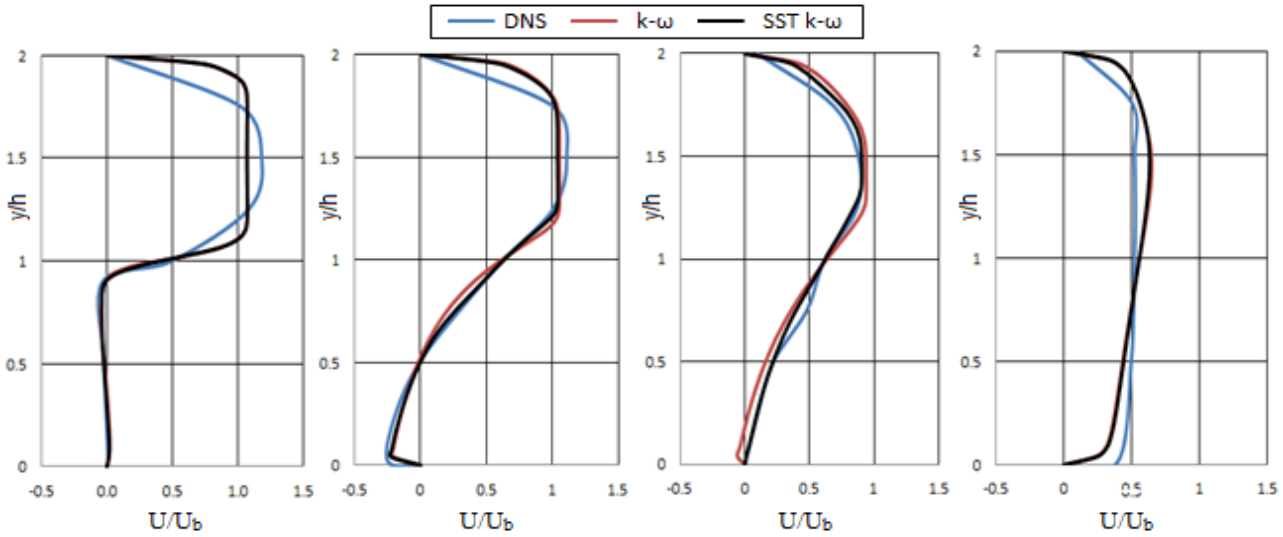

(a) *x/h* = 0.5 (b) *x/h* = 4 (c) *x/h* = 8 (d) *x/h* = 20

Figure 5. *U* velocity profiles at four positions.

In the first location of Fig. 5 the fully developed flow freely extends in the structure, while at *x/h* = 4 the reverse flow caused by the adverse pressure gradient can be observed. At the last location (*x/h* = 20), the decrease in the difference between the top and the bottom wall is observed, which is expected since the flow tends to equilibrium as it goes downstream, after the reattachment length. Although close to equilibrium, the flow is not fully developed.

Figure 6 shows velocity profiles in wall units at four positions after reattachment length. This velocity is calculated by the friction velocity, the formulas used in this paper for the construction of these graphs are shown below

$$u_t = \sqrt{\frac{\tau_w}{\rho}} \; ; \; u^+ = \frac{u}{u_t} \; ; \; y^+ = \frac{u_t}{\upsilon} y \tag{10}$$

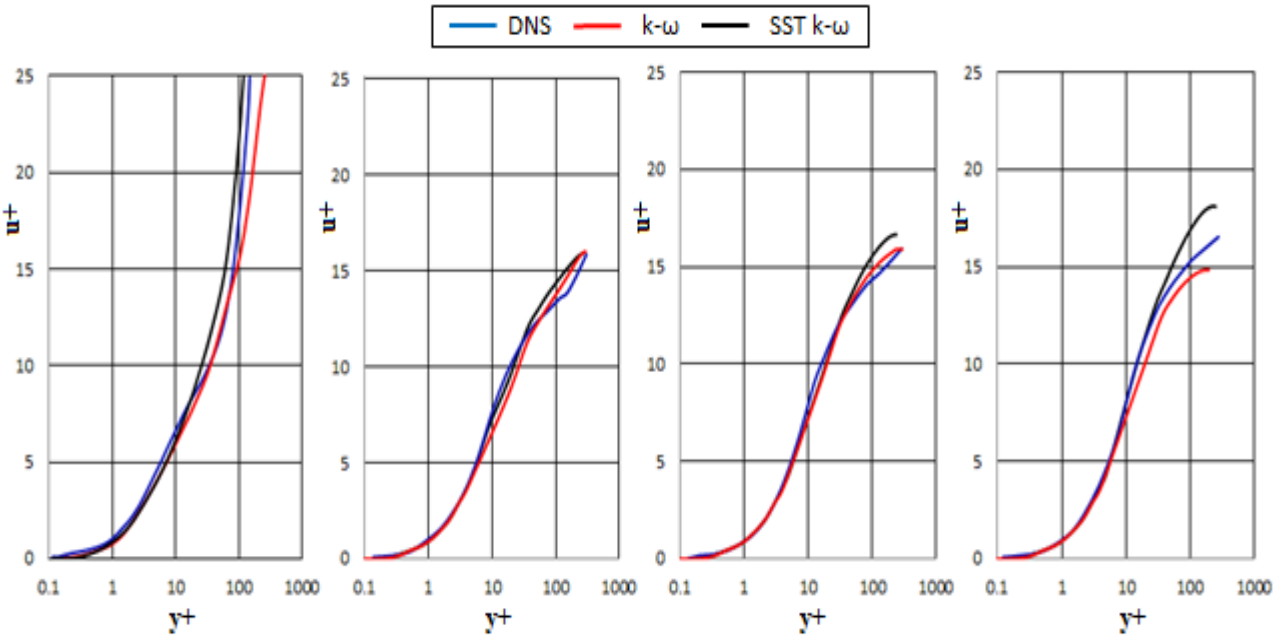

(a) x/h = 10 (b) x/h = 18 (c) x/h = 22 (d) x/h = 26

Figure 6. *U* velocity profiles in wall units at four positions.

In Fig. 6 it is shown that even at the most downstream location at x/h = 26 the fully developed velocity profile is not reached. The results found in this article using the *k-ω* and *SST k-ω* models are close to the data found by Kopera (2011) using *DNS*. As expected the results found when using SST *k-ω* model are slightly better than the results with *k-ω* model.

4.3 Pressure Distribuitions

The pressure distribution is analyzed by the pressure coefficient, given by

$$C_p = (P - P_0/0.5\rho U^2) \tag{11}$$

The term P_0 is the reference pressure at x = -4 m, y = 1.5 m.

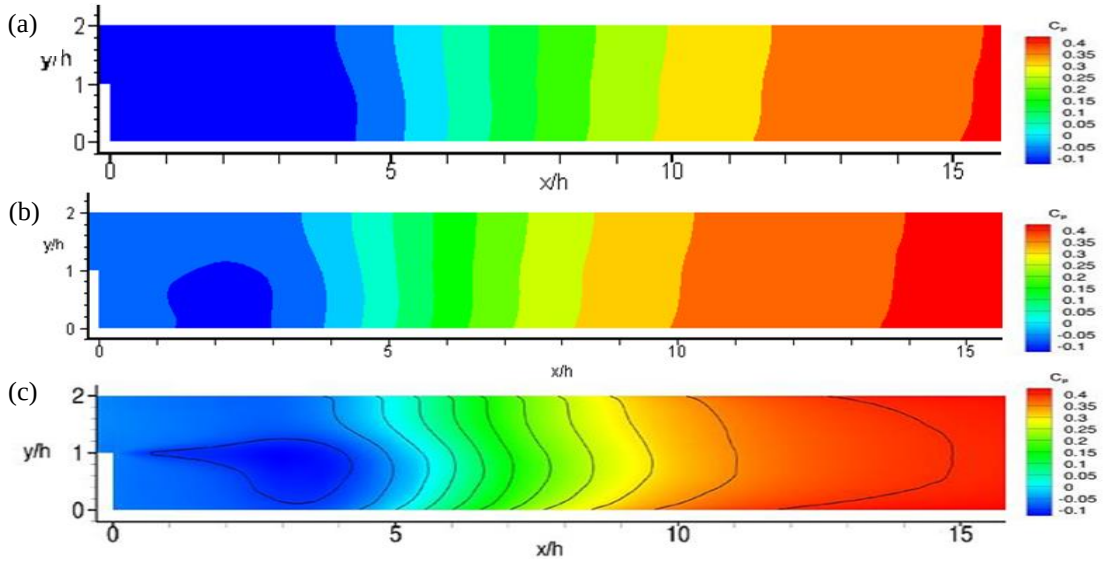

Figure 7. Mean static pressure coefficient contours. (a) *k-ω* model. (b) *SST k-ω* model. (c) *DNS*.

In Fig. 7 it can be clearly seen that there is a zone of pressure drop originating at the edge of the step and that in the case of the *k-ω* model it remains until approximately x = 2.98 m and in the *SST k-ω* model it remains until approximately x = 3.73 m, while in the *DNS* the zone of pressure drop ends around x = 5m.

Figure 8 shows static pressure at x/h = 0.5, x/h = 4, x/h = 8 and x/h = 20. The reference pressure P_w is taken at the top wall at each location. A difference is observed between the top wall pressure and the bottom wall pressure along the channel at the four locations. At x/h = 4 it is observed that the difference between the pressures $(P - P_w)$ is negative, while at x/h = 8 in the reattachment zone it is observed that the difference is positive. At x/h = 20 it is observed that the static pressure profile returns slowly towards a uniform distribution across the channel.

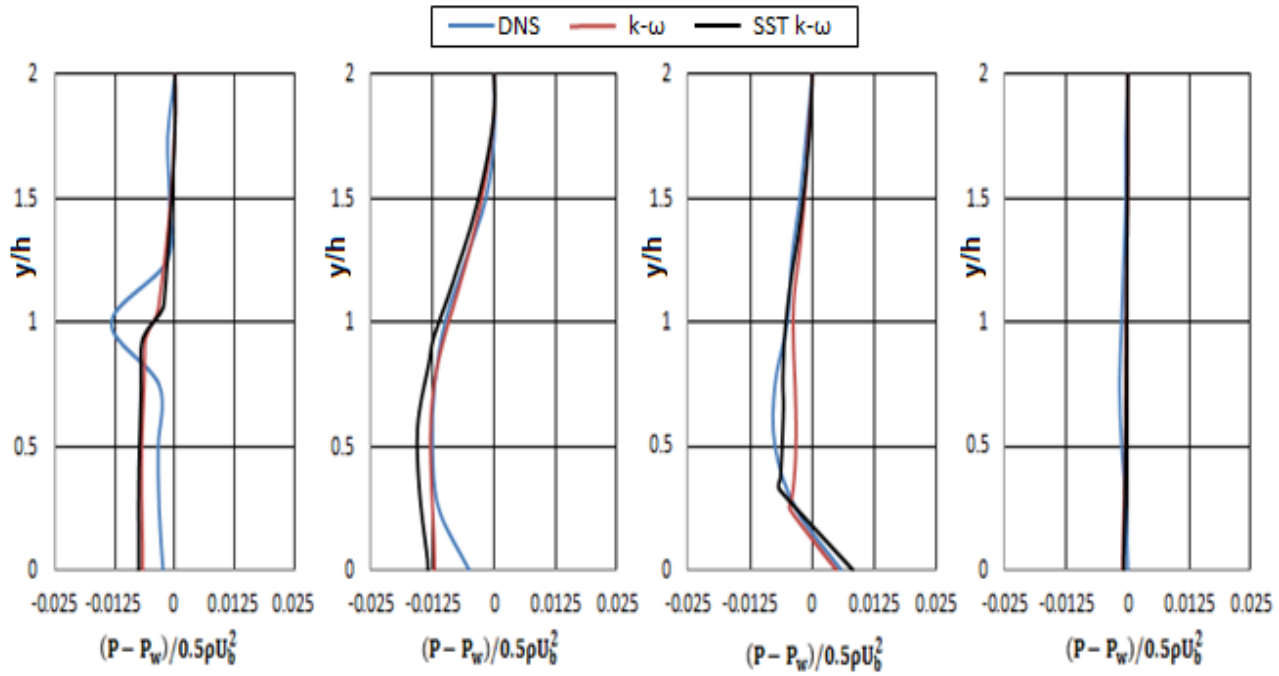

(a) x/h = 0.5 (b) x/h = 4 (c) x/h = 8 (d) x/h = 20

Figure 8. Static pressure at four positions.

5. CONCLUSIONS

In this work, two turbulence models based on Reynolds Averaged Navier-Stokes (*RANS*) equations were used to study the turbulent flow over a backward-facing step: *k-ω* and *SST k –ω* models. The results obtained were compared with the studies performed by Kopera (2011), using direct numerical simulation (*DNS*).

The results found in the two models are in agreement with the results found by Kopera (2011) and validated by the reattachment length, where X_R = 9.83 for E_R = 2 and Re = 9000 for *k-ω* model and X_R = 8.50 for E_R = 2 and Re = 9000 for *SST k-ω* model, both being close to the values found by Kopera (2011) for the case analyzed.

In both models used in the present work, the formation of a primary bubble in the region just after the step is visualized through the velocity streamlines, besides the presence of a secondary bubble near the edge of the step also presented in the results found by Kopera (2011).

In general, the results obtained using *SST k-ω* turbulence model are closer to the Kopera (2011) results when purchased from the results generated by the use of *k-ω* model, which was already expected since the *SST k-ω* model is an improvement of the standard *k-ω* model more efficient in cases with the presence of adverse pressure gradient and separation flow.

The great advantage of using the *k- ω* and *SST k-ω* models, when compared to the direct numerical simulation (*DNS*), is the lower computational cost and the shorter time required for the simulations. Thus, according to the results obtained, it is concluded that the *SST k-ω* model can be used in the simulated case of turbulent flow over a backward-facing step, as well as the standard *k-ω* model.

6. REFERENCES

Armaly, B. F., Dursts, F., J., Pereira, C. F., Schonung, B, 1983. Experimental and Theoretical Investigation of Backward-Facing Step Flow. Journal of Fluid Mechanics 01/1983; Page No: 473 - 496.

Cazalbou, J.B., Spalart, P.R., Bradshaw, P., 1993. On the Behavior of 2-Equation Models at the Edge of a Turbulent Region. Physics of Fluids, Vol. 6, No. 5, pp. 1797-1804.

Chitsomboon, T, 2011. Adjustment of kw SST Turbulence Model for an Improved Prediction of Stalls on Wind Turbine Blades. World Renewable Energy Congress-Sweden; 8-13 May; 2011; Linköping; Sweden; No. 057; Linköping University Electronic Press.

Hutchinson B. R., Raithby G. D, 1986. A Multigrid Method Based on the Additive Correction Strategy. Numerical Heat Transfer, p. 511-537.

Kopera, M. A, 2011. Direct numerical simulation of turbulent flow over a backward-facing step. University of Warwick, p. 1-18.

Lee, T., Mateescu, D., 1988. Experimental and Numerical Investigation of 2-D Backward-Facing Step Flow. Journal of Fluids and Structures (1998) 12, Page No: 703 – 716.

Leonard, B. P, 1979. A Stable and Accurate Convective Modelling Procedure Based on Quadratic Upstream Interpolation. Computer Methods in Applied Mechanics and Engineering, p. 59-98.

Menter, F. R, 1992. Influence of free stream values on *k-ω* turbulence model predictions. AIAA Journal, v. 30, n. 6, p. 1657-1659.

Menter, F. R, 1994. Two-Equation Eddy-Viscosity Turbulence Models for Engineering Applications. AIAA Jounal, Vol. 32, No. 8, pp. 1598-1605.

Miranda, W. R., 2014. Simulação Numérica de uma Bolha de Separação em Bordo Arredondado Utilizando Equações Médias de Reynolds. Departamento de Engenharia Mecânica, Instituto Militar de Engenharia – IME, Rio de Janeiro, Brasil.

Rezende, A.L.T., 2009. Análise numérica da bolha de separação do escoamento turbulento sobre placa plana fina inclinada. Departamento de Engenharia Mecânica, Pontifícia Universidade Católica, Rio de Janeiro.

Wilcox, David C, 1988. Reassessment of the Scale-Determining Equation for Advanced Scale Models. AIAA Journal v. 26, n. 11, p. 1299-1310.

Wilcox, David C, 1991. A half-century historical review of the k-w model. AIAA paper 91-0615.

Wilcox, D.C, 1998. Turbulence Modeling for CFD. Ed. DCW, Califórnia, EUA.

7. NOMENCLATURE

h	Height of the step, m
U	Mean inlet velocity, m/s
ρ	Density, Kg/m^3
υ	Kinematic viscosity, m^2/s
L_y	Height of the outlet chanel
μ	Molecular viscosity, kg/ms
p	Pressure, Pa
g_i	Acceleration of gravity
k	Turbulent Kinect energy, m^2/s^2
u_t	Friction velocity, m/s
τ_w	Wall shear stress, kg/ms^2
y	Distance to wall, m
ω	Specific turbulence dissipation rate, 1/s
ε	Turbulence dissipation rate, m^2/s^3

8. RESPONSIBILITY NOTICE

The authors are the only responsible for the printed material included in this paper.